Experimental Eye Research 131 (2015) 12–19

Contents lists available at ScienceDirect

Experimental Eye Research

journal homepage: www.elsevier.com/locate/yexer

Methods in eye research

Two methods to trace retinal ganglion cells with fluorogold: From the intact optic nerve or by stereotactic injection into the optic tract

Francisco M. Nadal-Nicolás [a, b], Manuel Salinas-Navarro [a, b], Manuel Vidal-Sanz [a, b], Marta Agudo-Barriuso [a, b, *]

[a] Instituto Murciano de Investigación Biosanitaria-Hospital Clínico Universitario Virgen de la Arrixaca (IMIB-VIRGEN DE LA ARRIXACA), Murcia, Spain
[b] Departamento de Oftalmología, Facultad de Medicina, Universidad de Murcia, Murcia, Spain

ARTICLE INFO

Article history:
Received 8 September 2014
Received in revised form
13 November 2014
Accepted in revised form 3 December 2014
Available online 4 December 2014

Keywords:
Tracing
Intact optic nerve
Stereotaxis
Optic tract
Brn3a
Retinal ganglion cells
Rat

1. Introduction

Retinal ganglion cells (RGCs) are the only afferent neurons of the retina. Their axons form the optic nerve and send visual information to the brain to perform image forming and non-image forming functions (Ramsey et al., 2013; Schmidt et al., 2011; Sefton et al., 2004).

RGCs are often used as a model to investigate the response of central nervous system neurons to different insults, such as axonal injury (Aguayo et al., 1987; Aviles-Trigueros et al., 2000; Galindo-Romero et al., 2011; Munz et al., 1985; Nadal-Nicolas et al., 2009; Parrilla-Reverter et al., 2009a, 2009b; Peinado-Ramon et al., 1996; Sasaki et al., 1996; Sobrado-Calvo et al., 2007; Vidal-Sanz et al., 2002; Whiteley et al., 1998), transient ischaemia (Aviles-Trigueros et al., 2003; Lafuente Lopez-Herrera et al., 2002; Mayor-Torroglosa et al., 2005) and to test neuroprotective therapies (Galindo-Romero et al., 2013; Lafuente et al., 2002; Parrilla-Reverter et al., 2009b; Peinado-Ramon et al., 1996; Sanchez-Migallon et al., 2011; Vidal-Sanz et al., 2000). RGCs are also the target of diseases such as glaucomatous optic neuropathies or retinal degenerations, and thus animal models mimicking these diseases are the subject of intensive research (Casson et al., 2004; Danias et al., 2006; Garcia-Ayuso et al., 2011, 2014; Marco-Gomariz et al., 2006; Salinas-Navarro et al., 2009a, 2010; Vidal-Sanz et al., 2012; Wang et al., 2003).

The majority of RGCs are located in the innermost layer of the retina, the ganglion cell layer, where most RGCs share location with the equally numerous population of displaced amacrine cells (Dräger and Olsen, 1981; Jeon et al., 1998; Perry, 1981), although a minute proportion have their RGC somata in the inner nuclear or inner plexiform layers of the retina, the so called displaced RGCs (Nadal-Nicolas et al., 2014). Thus, in order to study RGCs it is essential to specifically identify them. One well established method to label the majority of RGCs is tracing them from their main retinorecipient areas in the brain which in rodents are the superior colliculi (Linden and Perry, 1983; Salinas-Navarro et al., 2009b, 2009c; Thanos et al., 1987; Vidal-Sanz et al., 1988). Another tracing approach is from the optic nerve, with this method the whole retinofugal projection is identified (Lafuente Lopez-Herrera et al., 2002; Nadal-Nicolas et al., 2012; Salinas-Navarro et al., 2009b, 2009c).

Tracing from both superior colliculi can be achieved by i/multiple stereotactic injections (Barnstable and Drager, 1984; Siddiqui et al., 2014; Soto et al., 2008) which, if not done properly may lead to regions of the retina left untraced, or ii/by covering them with a gelatine sponge soaked in the tracer (Danias et al., 2002, 2006; Galindo-Romero et al., 2011; Nadal-Nicolas et al., 2009, 2012; Salinas-Navarro et al., 2009b; Salinas-Navarro et al. 2009c; Vidal-Sanz et al., 1988; Villegas-Perez et al., 1993, 1996). This latter approach involves removing the occipital cortex above the SC, and thus it is technically more demanding. Tracing from the optic nerve (ON) requires severing it and placing the tracer onto the ocular stump. This results in an axotomy of the RGC population (Fu et al., 2008; Nadal-Nicolas et al., 2012; Salinas-Navarro et al., 2009b,

* Corresponding author. Dpto Oftalmología, Facultad de Medicina, Campus Espinardo, Universidad de Murcia, 30100 Murcia, Spain.
E-mail address: martabar@um.es (M. Agudo-Barriuso).

http://dx.doi.org/10.1016/j.exer.2014.12.005
0014-4835/© 2014 The Authors. Published by Elsevier Ltd. This is an open access article under the CC BY-NC-ND license (http://creativecommons.org/licenses/by-nc-nd/3.0/).

2009c).

In the visual system fluorogold (FG) has become the tracer of choice for many laboratories. This compound is actively and retrogradely transported from the axons to the RGC somas where it accumulates without leaking (Schmued and Fallon, 1986; Wessendorf, 1991; reviewed in Kobbert et al., 2000). Thus, 3 days after its application on the optic nerve stump, all the RGCs are traced (Nadal-Nicolas et al., 2012; Salinas-Navarro et al., 2009b, 2009c), while when applied onto both SCi approximately one week is needed to label 98.4% and 97.8% of the RGC population in albino and pigmented rats, respectively (Danias et al., 2002; Salinas-Navarro et al., 2009b, 2009c).

Here, we describe two reliable, effective and straightforward methods to trace the rat RGC population with FG: i/from the intact optic nerve, that is without severing the optic nerve (Nadal-Nicolas et al., 2014), and; ii/by a single stereotactic injection in the optic tract.

2. Material and supplies

2.1. Supplies

Gelatine sponge (Spongostan Film, Ferrosan A/S, Denmark).

Sterile saline (0.9% NaCl in water. Sigma Aldrich, Alcobendas, Madrid, Spain).

Artificial eye tears (optional).

Dimethyl-sulfoxide (DMSO, Sigma Aldrich, Alcobendas, Madrid, Spain).

Non absorbable silk sterile sutures (4/0 and 6/0 with a circular needle 1/2 12 mm. Lorca Marín, Murcia, Spain).

Disposable syringe needles (25G, internal diameter 0.50 mm. B Braun, Barcelona, Spain). Surgical blades (size 15, Fisher Scientific, Madrid, Spain).

Fluorogold (2-Hydroxystilbene-4, 4-dicarboxamidine bismethanesulfonate, Fluorochrome, LLC, USA).

2.2. Equipment

Standard stereotaxic instrument frame (Stoelting Europe).

Custom made rat head holder.

Retractors (17008-07), forceps (11231-30), needle holder (12002-14), micro-scissors (15020-159) (Fine Science Tools, Heidelberg, Germany).

Hamilton syringe (5 μL Model 85 RN SYR) with removable needle (34/38 pst2 TapN) (Hamilton Company, purchased from Teknokroma, Spain).

2.3. Fluorogold preparation

Fluorogold (FG), was prepared at 6% concentration (w/v) in a solution of 10% DMSO- saline.

2.4. Experimental animals and anaesthesia

Two month old female albino Sprague Dawley (SD, 180–220 g body weight) rats were obtained from the University of Murcia breeding colony. All experimental procedures were carried out in accordance with the Association for Research in Vision and Ophthalmology and European Union guidelines for the use of animals in research and were approved by the Ethical and Animal Studies Committee of the University of Murcia (Spain).

A mixture of xylazine (10 mg/kg body weight; Rompun®; Bayer, Kiel, Germany) and ketamine (60 mg/kg body weight; Ketolar®; Pfizer, Alcobendas, Madrid, Spain) was used intraperitoneally.

During surgery eyes were maintained hydrated with saline. After surgery an ointment containing tobramicin (Tobrex; Alcon S.A., Barcelona, Spain) was applied on the cornea to prevent its desiccation.

3. Detailed methods

3.1. Tracing from the intact optic nerve (Fig. 1)

First, soak small stripes of gelatine sponge (~2.5 mm long, 1 mm wide) in the FG solution. In general this is done in a microtube.

On a rat head holder, hold a deeply anesthetized rat by its teeth and snout, face down.

Maintain the rat's eyes hydrated by applying topical saline or artificial eye tears.

Make a rostro-caudal incision in the skull skin.

Maintain the incision open with a fixating suture in the skin (4/0).

Using a surgical blade open an incision along the supraorbital rim.

The back of the eye is accessible now. Dissect and gently displace aside the glands. Then, with the forceps hold the posterior part of the superior rectus muscle and detach it, taking care not to break its anterior insertion to the sclera. A fixating suture (6/0) in the anterior part of muscle allows rotating the eye to expose the optic nerve.

Open the meninges longitudinally with the use of micro-scissors. The opening should start at 0.5 mm from the optic head and end approximately at 3–4 mm.

Take a piece of FG-soaked gelatine. If the stripe is covered by or wrapped in a drop of FG, get rid of this excess of FG by tapping the stripe onto the dry walls of the microtube.

Wrap the optic nerve with a stripe of FG-soaked gelatine sponge. It is important to place the sponge at 1 mm from the optic head (Fig. 1 A).

Remove the fixating sutures and close the head wound with a 4/0 suture.

Check the eye fundus to verify that the retinal circulation is preserved.

Apply ointment on both eyes.

Animals are sacrificed 3 days later.

3.2. Tracing from the optic tract: stereotaxis (Fig. 2)

Position a deeply anesthetized rat on the stereotaxic frame.

Maintain the rat's eyes hydrated by applying topical saline or artificial eye tears.

Make a rostro-caudal incision in the skull skin.

Maintain the incision open using retractors.

Clean the skull with a cotton bud.

Mark with a permanent pen marker the position of the craneotomy using bregma coordinates (mm) rostro-caudal: −5.2, medio-lateral: ±3.65.

To perforate the skull, use a needle (25G): rotate it left-right right-left (see panel D in Fig. 2).

Make a small hole on the duramater puncturing it with the needle tip.

Fix the Hamilton syringe to the stereotaxic frame and load it with fluorogold.

Insert the Hamilton needle into the craniotomy.

Lower the Hamilton slowly till reaching the injection point. The dorso-ventral coordinates are −5.7.

Inject 1 μl of FG, very slowly. Wait 30 s before lifting the syringe.

Close the head wound with a 4/0 suture.

Apply ointment on both eyes.

Animals are sacrificed 7 days later.

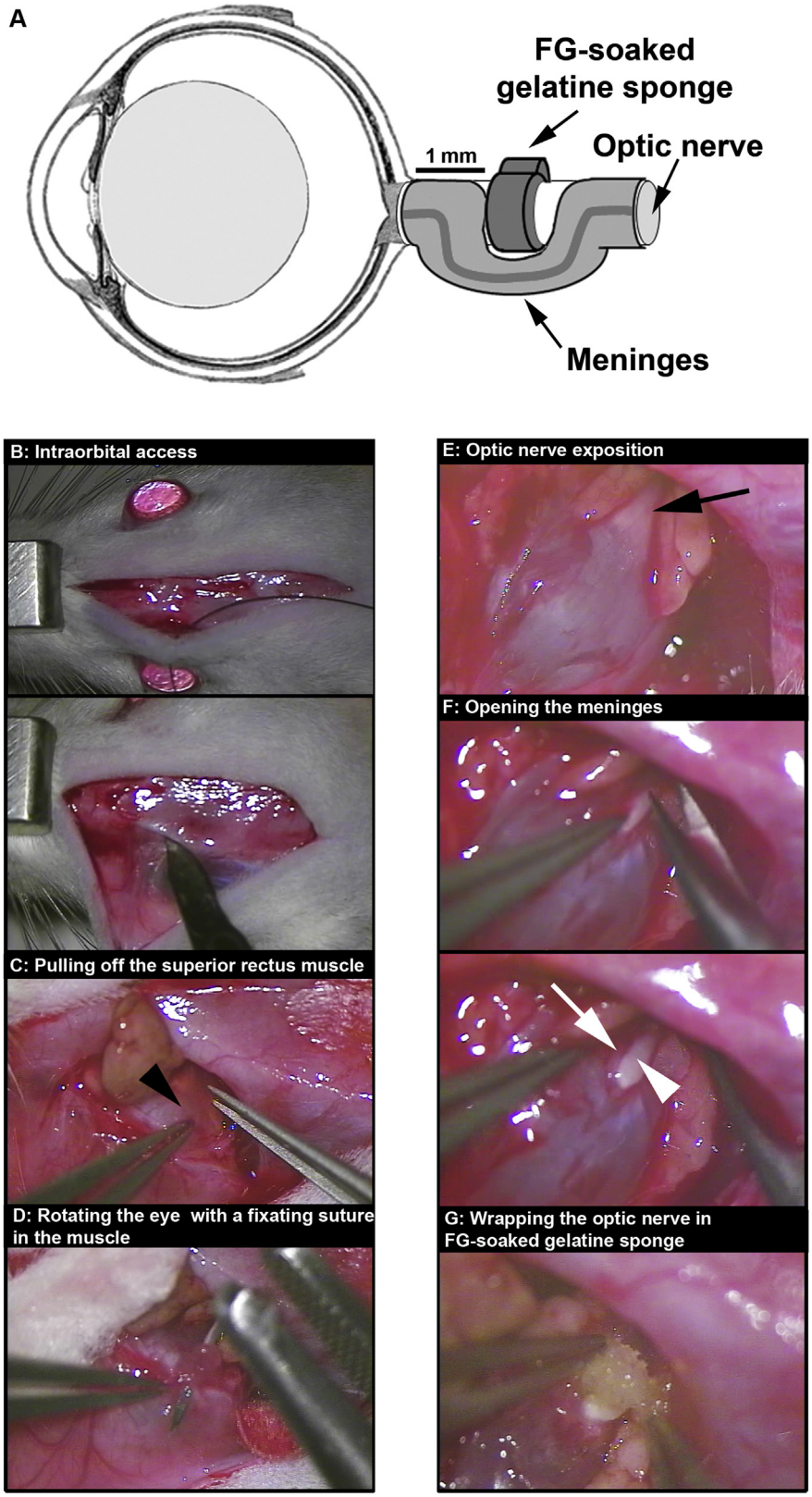


Fig. 1. Method to trace from the optic nerve without axotomy. **A**: Drawing depicting the experimental approach. The eye scheme is a modification from Ramsey et al. (2013). **B**–**G**: Images summarizing the main steps during the surgery. Black arrow head: superior rectus muscle. Black arrow: optic nerve. White arrow: meninges. White arrow head: exposed optic nerve.

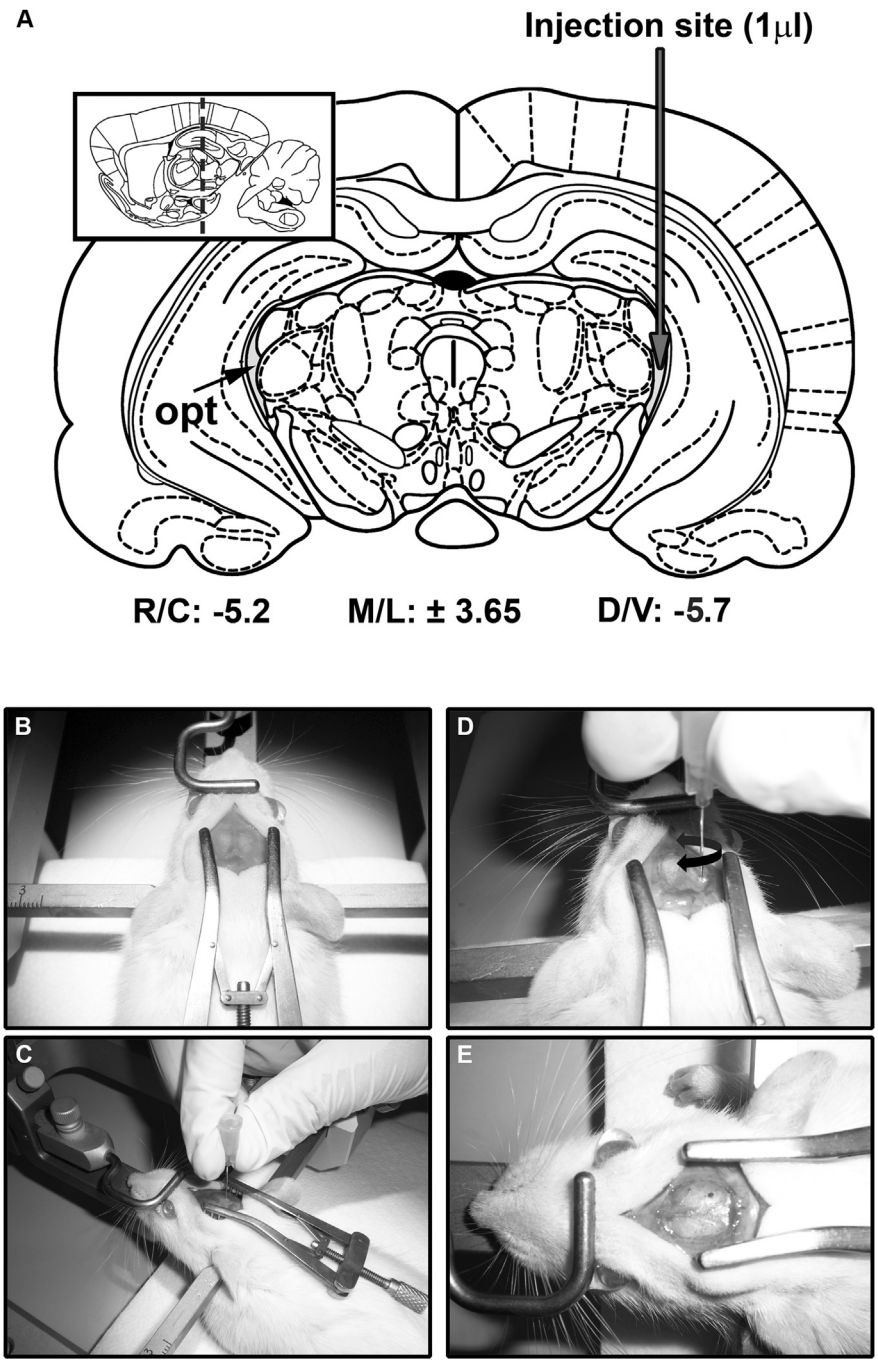


Fig. 2. Stereotactic injection in the optic tract. **A**: Coronal brain rat section showing the injection site. Plate 40 from "The rat brain stereotaxic coordinates" (Paxinos and Watson, 1998). Below are shown the rostro-caudal (R/C), medio-lateral (M/L) and dorso-ventral (D/V) coordinates from Bregma. The insert on the top is the sagittal section (Plate 86) corresponding approximately (±3.40) to the actual mediolateral position (±3.65). Reproduced with permission ©Elsevier. opt: optic tract. **B**–**E**: Images summarizing the main steps of the procedure.

3.3. Results

Three experimental groups were done: i/tracing by applying a pledge of gelatine foam soaked on FG onto the surface of both superior colliculi. This is a tracing technique standardized in our lab (Parrilla-Reverter et al., 2009b; Peinado-Ramon et al., 1996; Salinas-Navarro et al., 2009c; Villegas-Perez et al., 1996) and thus, this group served as control of the optic nerve tracing, and stereotactic tracing (Fig. 3 **top, A-C′**); ii/tracing from the optic nerve as described in point 3.1 (Fig. 3 **middle, D-F′**), and iii/tracing from the optic tract using a stereotactic injection as explained in point 3.2 (Fig. 3 **bottom, G-I′**).

In all retinas, Brn3a, a transcription factor specifically expressed by healthy RGCs (Galindo-Romero et al., 2011, 2013; Nadal-Nicolas et al., 2009, 2012, 2014; Sanchez-Migallon et al., 2011), was immunodetected as previously reported (Nadal-Nicolas et al., 2009). Brn3a detection served as internal control of the population of RGCs after tracing (Fig. 3 A′-I′). Then, using automated counting routines developed by our lab the total number of RGCs was quantified (Table 1) and their distribution in the retina

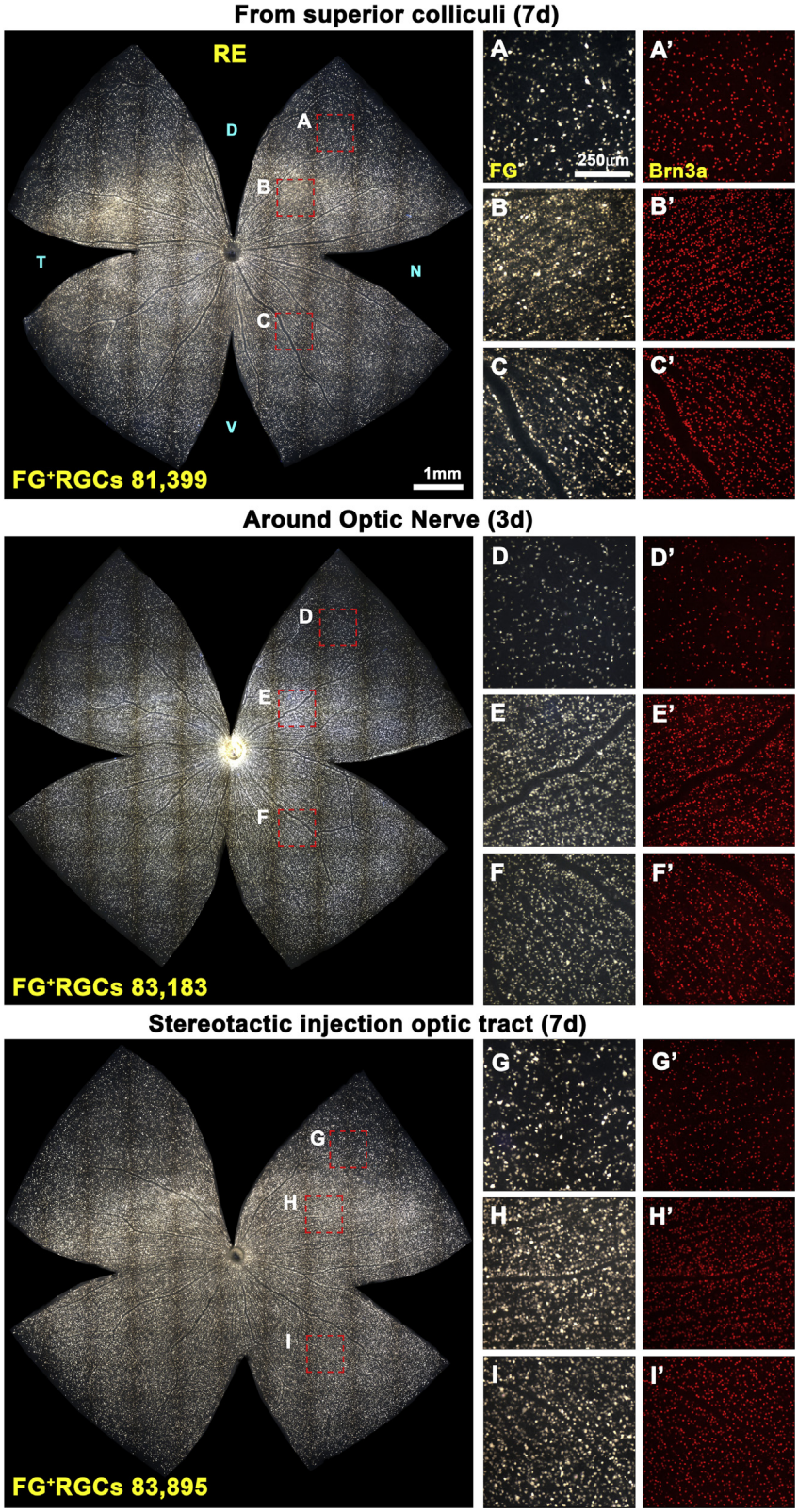


Fig. 3. FG tracing from the intact optic nerve or from the optic tract results in the labelling of all RGCs. Retinal photomontages showing FG-traced RGCs 7 days after applying FG onto the surface of both superior colliculi (top, tracing control), 3 days after wrapping the optic nerve in FG-soaked gelatine sponge (middle) or 7 days after the stereotactic injection of the tracer in the optic tract (bottom). **A**–**C**, **D**–**F**, **G**–**H**, magnifications taken from the areas framed in the photomontages showing in more detail the traced RGCs. **A′**–**C′**, **D′**–**F′**, **G′**–**H′**: Brn3a^{+}RGCs in the same magnifications. At the bottom of each photomontage is shown the number of FG-traced RGCs counted in it. D: dorsal, V: ventral, N: nasal, T: temporal.

Table 1
Total number of RGCs.

Tracer application		Total number of	
		FG$^+$RGCs	Brn3a$^+$RGCs
Superior colliculi ($n = 4$ retinas)	Mean	81,848*	82,443§
	SD	1275	1634
Around optic nerve ($n = 11$ retinas)	Mean	82,881*	81,311§
	SD	1691	1345
Optic tract (stereotaxis) ($n = 12$ retinas)	Mean	81,398*	81,908§
	SD	4284	2128

Mean ± standard deviation of FG$^+$RGCs in retinas traced either by applying FG onto the superior colliculi, from the optic nerve or by stereotactic injection in the optic tract. In these same retinas, Brn3a$^+$RGCs were also quantified. *,§There were no statistically significant differences in the number of FG-traced or Brn3a$^+$RGCs among the three groups (ANOVA $p > 0.05$).

visualized using isodensity maps (Fig. 4), as previously described (Nadal-Nicolas et al., 2009; Salinas-Navarro et al., 2009c).

As shown in Table 1, the total numbers of FG$^+$RGCs and Brn3a$^+$RGCs were comparable in the three tracing groups. After tracing from the optic nerve or the optic tract (Fig. 3), labelled RGCs distribute across the entire retina with the same pattern as that observed when the tracer is applied to both SCi. RGCs adopt a form of regional specialization resembling a horizontal visual streak in the dorsal retina along the naso-temporal axis with highest density clusters in the superotemporal quadrant, as previously described (Nadal-Nicolas et al., 2009; Ortin-Martinez et al., 2010; Salinas-Navarro et al., 2009c). Notice that tracing from the ON results in a slight tracer accumulation around the optic disk (Fig. 3E). This accumulation is minimised by placing the gelatine-sponge at 1 mm

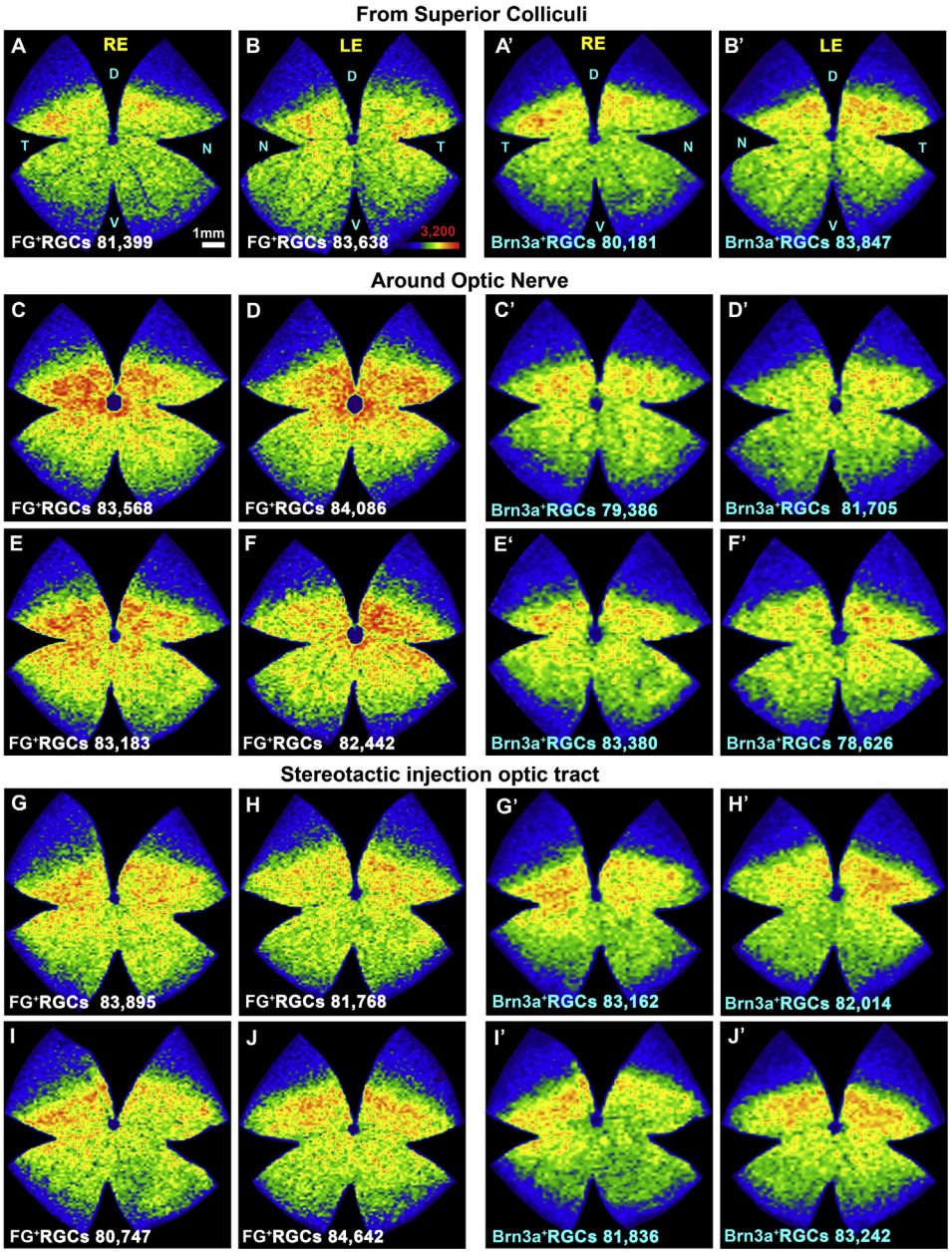


Fig. 4. Retinal distribution of FG-traced RGCs and Brn3a$^+$RGCs in retinas traced from the intact optic nerve and from the optic tract. Isodensity maps showing the topography of RGCs in two retinas traced from the superior colliculi (**A**–**B**, tracing control), and four retinas traced from the optic nerve (**C**–**F**), or from the optic tract (**G**–**J**). **A′**–**J′** isodensity maps showing the distribution of Brn3a$^+$RGCs in the same retinas as **A**–**J**. Note that isodensity maps A–A′, E–E′ and G–G′ are from the retinas shown in Fig. 3, respectively. Colour scale density is shown in **B**, and goes from 0 RGCs/mm^2 (purple) to ≥3200 RGCs/mm^2 (red). At the bottom of each map is shown the number of RGCs (FG$^+$ or Brn3a$^+$) counted in the retina wherefrom each map was created. D: dorsal, V: ventral, N: nasal, T: temporal. RE: right eye. LE: left eye.

from the optic disk.

Detailed isodensity maps (Fig. 4), demonstrate that the distribution of FG^+RGCs is comparable in the three experimental groups. These images provide further evidence that the application of the tracer around the optic nerve or on the optic tract results in the labelling of the whole RGC population. $Brn3a^+$RGCs isodensity maps from the same retinas also disclose that neither tracing method causes a local or diffuse RGC loss, in agreement with the quantitative data (Table 1).

4. Potential pitfalls and troubleshooting

The methods described here require an intact retinofugal system and thus could not be used in experiments with previous lesion to the ON. Besides, FG transport relies on a competent retrograde axonal transport and therefore these methods cannot be used in experimental situations with an impaired axonal transport.

Fluorogold is dissolved in DMSO, which has been recently reported to be neurotoxic (Galvao et al., 2014). Thus, the application of this solvent either in the SC, optic nerve or optic tract may cause a deleterious effect that may trigger changes in gene or protein expression. Hence, even though at the survival intervals of our study there was not RGC loss, retrogradely traced retinas and their brains (see Sections 4.1 and 4.2) should be used for anatomical rather than for molecular studies.

FG is not a persistent neuronal tracer (Kobbert et al., 2000) and within four to five weeks after application to both SCi or to the lateral rectus muscle of the eye the numbers of FG-labelled RGCs or abducens motoneurons, respectively, diminish progressively with time (Gomez-Ramirez et al., 1999; Selles-Navarro et al., 1996). Importantly, in these studies there was not an observable toxic effect although the tracer was dissolved in DMSO. This was demonstrated by a successful tracing of the neurons after a second application of FG several months after the first tracing (Gomez-Ramirez et al., 1999).

Counting FG-labelled RGCs after retinal injury may require experience and expertise to count manually and distinguish RGCs from phagocytic microglia that become transcellularly labelled as they clear the detritus of the traced RGCs (Galindo-Romero et al., 2013; Nadal-Nicolas et al., 2009; Peinado-Ramon et al., 1996; Sanchez-Migallon et al., 2011; Thanos et al., 1992).

Finally, if we compare the reliability of both methods, tracing from the optic nerve is more consistent (less variability) than tracing from the optic tract.

4.1. Tracing from the intact optic nerve

When using this approach, the orbital contents are intensely labelled with FG. Therefore the motoneuron nuclei in the brain innervating the extraocular muscles would probably become retrogradelly traced. This should be taken into account if the brains are going to be studied.

Even though with this approach the optic nerve is not directly injured, it is, nevertheless, manipulated. Thus, when opening the meninges and wrapping the optic nerve with the FG-soaked gelatine sponge, care has to be taken to avoid damaging the nerve and/or the vasculature. Damage to the nerve would result in a typical sectorial RGC loss circumscribed to the regions of the retina that are the origin of the injured axons. If the meninges were to be severed or damaged, a retinal ischaemia will follow, and this would also result in retinal degeneration (Lafuente Lopez-Herrera et al., 2002; Mayor-Torroglosa et al., 2005). Thus, it is very important to inspect the eye fundus after surgery to ascertain normal retinal blood supply.

4.2. Tracing from the optic tract

If the brain of traced rats is going to be examined, it is important to bear in mind that to reach the injection point the needle passes through the cortex and other structures placed above the optic tract. As result, they may be damaged and/or spuriously labelled with the tracer. In addition, once the injection point is reached, a small volume of liquid is released in the brain parenchyma, and this might harm the optic tract and neighbouring structures.

In relation to this, the retinal projections in the optic tract might, therefore, be injured causing an intracraneal axotomy to RGCs. However the possibility, it should be noted that seven days after the tracing, no RGC death was observed.

Funding

This work was supported by grants from: Instituto de Salud Carlos III (ISCIII) -FEDER "Una manera de hacer Europa" -Spanish Ministry of Economy and Competitivenes: PI13/00643; Red Temática de Investigación Cooperativa en Oftalmología RETICS: RD12/0034/0014 and Spanish Ministry of Economy and Competitiveness: SAF-2012-38328.

Acknowledgements

We are very grateful to Prof. Margarita Martínez de la Torre Fox (Dpto Anatomía y Psicobiología Humana, Murcia University, Murcia, Spain) for lending us the stereotaxic frame.

References

Aguayo, A.J., Vidal-Sanz, M., Villegas-Perez, M.P., Bray, G.M., 1987. Growth and connectivity of axotomized retinal neurons in adult rats with optic nerves substituted by PNS grafts linking the eye and the midbrain. Ann. N. Y. Acad. Sci. 495, 1–9.

Aviles-Trigueros, M., Mayor-Torroglosa, S., Garcia-Aviles, A., Lafuente, M.P., Rodriguez, M.E., Miralles-Imperial, J., Villegas-Perez, M.P., Vidal-Sanz, M., 2003. Transient ischemia of the retina results in massive degeneration of the retinotectal projection: long-term neuroprotection with brimonidine. Exp. Neurol. 184, 767–777.

Aviles-Trigueros, M., Sauve, Y., Lund, R.D., Vidal-Sanz, M., 2000. Selective innervation of retinorecipient brainstem nuclei by retinal ganglion cell axons regenerating through peripheral nerve grafts in adult rats. J. Neurosci. 20, 361–374.

Barnstable, C.J., Drager, U.C., 1984. Thy-1 antigen: a ganglion cell specific marker in rodent retina. Neuroscience 11, 847–855.

Casson, R.J., Chidlow, G., Wood, J.P., Vidal-Sanz, M., Osborne, N.N., 2004. The effect of retinal ganglion cell injury on light-induced photoreceptor degeneration. Investig. Ophthalmol. Vis. Sci. 45, 685–693.

Danias, J., Shen, F., Goldblum, D., Chen, B., Ramos-Esteban, J., Podos, S.M., Mittag, T., 2002. Cytoarchitecture of the retinal ganglion cells in the rat. Investig. Ophthalmol. Vis. Sci. 43, 587–594.

Danias, J., Shen, F., Kavalarakis, M., Chen, B., Goldblum, D., Lee, K., Zamora, M.F., Su, Y., Brodie, S.E., Podos, S.M., Mittag, T., 2006. Characterization of retinal damage in the episcleral vein cauterization rat glaucoma model. Exp. Eye Res. 82, 219–228.

Dräger, U.C., Olsen, J.F., 1981. Ganglion cell distribution in the retina of the mouse. Investig. Ophthalmol. Vis. Sci. 20, 285–293.

Fu, Q.L., Hu, B., Wu, W., Pepinsky, R.B., Mi, S., So, K.F., 2008. Blocking LINGO-1 function promotes retinal ganglion cell survival following ocular hypertension and optic nerve transection. Investig. Ophthalmol. Vis. Sci. 49, 975–985.

Galindo-Romero, C., Aviles-Trigueros, M., Jimenez-Lopez, M., Valiente-Soriano, F.J., Salinas-Navarro, M., Nadal-Nicolas, F., Villegas-Perez, M.P., Vidal-Sanz, M., Agudo-Barriuso, M., 2011. Axotomy-induced retinal ganglion cell death in adult mice: quantitative and topographic time course analyses. Exp. Eye Res. 92, 377–387.

Galindo-Romero, C., Valiente-Soriano, F.J., Jimenez-Lopez, M., Garcia-Ayuso, D., Villegas-Perez, M.P., Vidal-Sanz, M., Agudo-Barriuso, M., 2013. Effect of brain-derived neurotrophic factor on mouse axotomized retinal ganglion cells and phagocytic microglia. Investig. Ophthalmol. Vis. Sci. 54, 974–985.

Galvao, J., Davis, B., Tilley, M., Normando, E., Duchen, M.R., Cordeiro, M.F., 2014. Unexpected low-dose toxicity of the universal solvent DMSO. FASEB J. 28, 1317–1330.

Garcia-Ayuso, D., Salinas-Navarro, M., Agudo-Barriuso, M., Alarcon-Martinez, L., Vidal-Sanz, M., Villegas-Perez, M.P., 2011. Retinal ganglion cell axonal compression by retinal vessels in light-induced retinal degeneration. Mol. Vis.

17, 1716–1733.
Garcia-Ayuso, D., Salinas-Navarro, M., Nadal-Nicolas, F.M., Ortin-Martinez, A., Agudo-Barriuso, M., Vidal-Sanz, M., Villegas-Perez, M.P., 2014. Sectorial loss of retinal ganglion cells in inherited photoreceptor degeneration is due to RGC death. Br. J. Ophthalmol. 98, 396–401.
Gomez-Ramirez, A.M., Villegas-Perez, M.P., Miralles, D.I., Salvador-Silva, M., Vidal-Sanz, M., 1999. Effects of intramuscular injection of botulinum toxin and doxorubicin on the survival of abducens motoneurons. Investig. Ophthalmol. Vis. Sci. 40, 414–424.
Jeon, C.J., Strettoi, E., Masland, R.H., 1998. The major cell populations of the mouse retina. J. Neurosci. 18, 8936–8946.
Kobbert, C., Apps, R., Bechmann, I., Lanciego, J.L., Mey, J., Thanos, S., 2000. Current concepts in neuroanatomical tracing. Prog. Neurobiol. 62, 327–351.
Lafuente Lopez-Herrera, M.P., Mayor-Torroglosa, S., Miralles, D.I., Villegas-Perez, M.P., Vidal-Sanz, M., 2002. Transient ischemia of the retina results in altered retrograde axoplasmic transport: neuroprotection with brimonidine. Exp. Neurol. 178, 243–258.
Lafuente, M.P., Villegas-Perez, M.P., Mayor, S., Aguilera, M.E., Miralles-Imperial, J., Vidal-Sanz, M., 2002. Neuroprotective effects of brimonidine against transient ischemia-induced retinal ganglion cell death: a dose response in vivo study. Exp. Eye Res. 74, 181–189.
Linden, R., Perry, V.H., 1983. Massive retinotectal projection in rats. Brain Res. 272, 145–149.
Marco-Gomariz, M.A., Hurtado-Montalban, N., Vidal-Sanz, M., Lund, R.D., Villegas-Perez, M.P., 2006. Phototoxic-induced photoreceptor degeneration causes retinal ganglion cell degeneration in pigmented rats. J. Comp. Neurol. 498, 163–179.
Mayor-Torroglosa, S., De la Villa, P., Rodriguez, M.E., Lopez-Herrera, M.P., Aviles-Trigueros, M., Garcia-Aviles, A., de Imperial, J.M., Villegas-Perez, M.P., Vidal-Sanz, M., 2005. Ischemia results 3 months later in altered ERG, degeneration of inner layers, and deafferented tectum: neuroprotection with brimonidine. Investig. Ophthalmol. Vis. Sci. 46, 3825–3835.
Munz, M., Rasminsky, M., Aguayo, A.J., Vidal-Sanz, M., Devor, M.G., 1985. Functional activity of rat brainstem neurons regenerating axons along peripheral nerve grafts. Brain Res. 340, 115–125.
Nadal-Nicolas, F.M., Jimenez-Lopez, M., Salinas-Navarro, M., Sobrado-Calvo, P., Alburquerque-Bejar, J.J., Vidal-Sanz, M., Agudo-Barriuso, M., 2012. Whole number, distribution and co-expression of brn3 transcription factors in retinal ganglion cells of adult albino and pigmented rats. PLoS One 7, e49830.
Nadal-Nicolas, F.M., Jimenez-Lopez, M., Sobrado-Calvo, P., Nieto-Lopez, L., Canovas-Martinez, I., Salinas-Navarro, M., Vidal-Sanz, M., Agudo, M., 2009. Brn3a as a marker of retinal ganglion cells: qualitative and quantitative time course studies in naive and optic nerve-injured retinas. Investig. Ophthalmol. Vis. Sci. 50, 3860–3868.
Nadal-Nicolas, F.M., Salinas-Navarro, M., Jimenez-Lopez, M., Sobrado-Calvo, P., Villegas-Perez, M.P., Vidal-Sanz, M., Agudo-Barriuso, M., 2014. Displaced retinal ganglion cells in albino and pigmented rats. Front. Neuroanat. 6 (8), 99. http://dx.doi.org/10.3389/fnana.2014.00099 eCollection 2014.
Ortin-Martinez, A., Jimenez-Lopez, M., Nadal-Nicolas, F.M., Salinas-Navarro, M., Alarcon-Martinez, L., Sauve, Y., Villegas-Perez, M.P., Vidal-Sanz, M., Agudo-Barriuso, M., 2010. Automated quantification and topographical distribution of the whole population of S- and L-cones in adult albino and pigmented rats. Investig. Ophthalmol. Vis. Sci. 51, 3171–3183.
Parrilla-Reverter, G., Agudo, M., Nadal-Nicolas, F., Alarcon-Martinez, L., Jimenez-Lopez, M., Salinas-Navarro, M., Sobrado-Calvo, P., Bernal-Garro, J.M., Villegas-Perez, M.P., Vidal-Sanz, M., 2009a. Time-course of the retinal nerve fibre layer degeneration after complete intra-orbital optic nerve transection or crush: a comparative study. Vis. Res. 49, 2808–2825.
Parrilla-Reverter, G., Agudo, M., Sobrado-Calvo, P., Salinas-Navarro, M., Villegas-Perez, M.P., Vidal-Sanz, M., 2009b. Effects of different neurotrophic factors on the survival of retinal ganglion cells after a complete intraorbital nerve crush injury: a quantitative in vivo study. Exp. Eye Res. 89, 32–41.
Paxinos, G., Watson, C., 1998. The Rat Brain in Stereotaxic Coordinates, Fourth ed. Academic Press Inc (Copyright Elsevier).
Peinado-Ramon, P., Salvador, M., Villegas-Perez, M.P., Vidal-Sanz, M., 1996. Effects of axotomy and intraocular administration of NT-4, NT-3, and brain-derived neurotrophic factor on the survival of adult rat retinal ganglion cells. A quantitative in vivo study. Investig. Ophthalmol. Vis. Sci. 37, 489–500.
Perry, V.H., 1981. Evidence for an amacrine cell system in the ganglion cell layer of the rat retina. Neuroscience 6, 931–944.
Ramsey, D.J., Ramsey, K.M., Vavvas, D.G., 2013. Genetic advances in ophthalmology: the role of melanopsin-expressing, intrinsically photosensitive retinal ganglion cells in the circadian organization of the visual system. Semin. Ophthalmol. 28, 406–421.
Salinas-Navarro, M., Alarcon-Martinez, L., Valiente-Soriano, F.J., Jimenez-Lopez, M., Mayor-Torroglosa, S., Aviles-Trigueros, M., Villegas-Perez, M.P., Vidal-Sanz, M., 2010. Ocular hypertension impairs optic nerve axonal transport leading to progressive retinal ganglion cell degeneration. Exp. Eye Res. 90, 168–183.
Salinas-Navarro, M., Alarcon-Martinez, L., Valiente-Soriano, F.J., Ortin-Martinez, A., Jimenez-Lopez, M., Aviles-Trigueros, M., Villegas-Perez, M.P., De la Villa, P., Vidal-Sanz, M., 2009a. Functional and morphological effects of laser-induced ocular hypertension in retinas of adult albino Swiss mice. Mol. Vis. 15, 2578–2598.
Salinas-Navarro, M., Jimenez-Lopez, M., Valiente-Soriano, F.J., Alarcon-Martinez, L., Aviles-Trigueros, M., Mayor, S., Holmes, T., Lund, R.D., Villegas-Perez, M.P., Vidal-Sanz, M., 2009b. Retinal ganglion cell population in adult albino and pigmented mice: a computerized analysis of the entire population and its spatial distribution. Vis. Res. 49, 637–647.
Salinas-Navarro, M., Mayor-Torroglosa, S., Jimenez-Lopez, M., Aviles-Trigueros, M., Holmes, T.M., Lund, R.D., Villegas-Perez, M.P., Vidal-Sanz, M., 2009c. A computerized analysis of the entire retinal ganglion cell population and its spatial distribution in adult rats. Vis. Res. 49, 115–126.
Sanchez-Migallon, M.C., Nadal-Nicolas, F.M., Jimenez-Lopez, M., Sobrado-Calvo, P., Vidal-Sanz, M., Agudo-Barriuso, M., 2011. Brain derived neurotrophic factor maintains Brn3a expression in axotomized rat retinal ganglion cells. Exp. Eye Res. 92, 260–267.
Sasaki, H., Coffey, P., Villegas-Perez, M.P., Vidal-Sanz, M., Young, M.J., Lund, R.D., Fukuda, Y., 1996. Light induced EEG desynchronization and behavioral arousal in rats with restored retinocollicular projection by peripheral nerve graft. Neurosci. Lett. 218, 45–48.
Schmidt, T.M., Chen, S.K., Hattar, S., 2011. Intrinsically photosensitive retinal ganglion cells: many subtypes, diverse functions. Trends Neurosci. 34, 572–580.
Schmued, L.C., Fallon, J.H., 1986. Fluoro-Gold: a new fluorescent retrograde axonal tracer with numerous unique properties. Brain Res. 377, 147–154.
Sefton, A.J., Dreher, B., Hattar, S., 2004. Visual system. In: Paxinos, G. (Ed.), The Rat Nervous System, Third ed., vol. 32. Elsevier, USA, pp. 1083–1165.
Selles-Navarro, I., Villegas-Perez, M.P., Salvador-Silva, M., Ruiz-Gomez, J.M., Vidal-Sanz, M., 1996. Retinal ganglion cell death after different transient periods of pressure-induced ischemia and survival intervals. A quantitative in vivo study. Investig. Ophthalmol. Vis. Sci. 37, 2002–2014.
Siddiqui, A.M., Sabljic, T.F., Koeberle, P.D., Ball, A.K., 2014. Downregulation of BM88 after optic nerve injury. Investig. Ophthalmol. Vis. Sci. 55, 1919–1929.
Sobrado-Calvo, P., Vidal-Sanz, M., Villegas-Perez, M.P., 2007. Rat retinal microglial cells under normal conditions, after optic nerve section, and after optic nerve section and intravitreal injection of trophic factors or macrophage inhibitory factor. J. Comp. Neurol. 501, 866–878.
Soto, I., Oglesby, E., Buckingham, B.P., Son, J.L., Roberson, E.D., Steele, M.R., Inman, D.M., Vetter, M.L., Horner, P.J., Marsh-Armstrong, N., 2008. Retinal ganglion cells downregulate gene expression and lose their axons within the optic nerve head in a mouse glaucoma model. J. Neurosci. 28, 548–561.
Thanos, S., Vidal-Sanz, M., Aguayo, A.J., 1987. The use of rhodamine-B-isothiocyanate (RITC) as an anterograde and retrograde tracer in the adult rat visual system. Brain Res. 406, 317–321.
Thanos, S., Pavlidis, C., Mey, J., Thiel, H.J., 1992. Specific transcellular staining of microglia in the adult rat after traumatic degeneration of carbocyanine-filled retinal ganglion cells. Exp. Eye Res. 55, 101–117.
Vidal-Sanz, M., Aviles-Trigueros, M., Whiteley, S.J., Sauve, Y., Lund, R.D., 2002. Reinnervation of the pretectum in adult rats by regenerated retinal ganglion cell axons: anatomical and functional studies. Prog. Brain Res. 137, 443–452.
Vidal-Sanz, M., Lafuente, M., Sobrado-Calvo, P., Selles-Navarro, I., Rodriguez, E., Mayor-Torroglosa, S., Villegas-Perez, M.P., 2000. Death and neuroprotection of retinal ganglion cells after different types of injury. Neurotox. Res. 2, 215–227.
Vidal-Sanz, M., Salinas-Navarro, M., Nadal-Nicolas, F.M., Alarcon-Martinez, L., Valiente-Soriano, F.J., de Imperial, J.M., Aviles-Trigueros, M., Agudo-Barriuso, M., Villegas-Perez, M.P., 2012. Understanding glaucomatous damage: anatomical and functional data from ocular hypertensive rodent retinas. Prog. Retin. Eye Res. 31, 1–27.
Vidal-Sanz, M., Villegas-Perez, M.P., Bray, G.M., Aguayo, A.J., 1988. Persistent retrograde labeling of adult rat retinal ganglion cells with the carbocyanine dye dil. Exp. Neurol. 102, 92–101.
Villegas-Perez, M.P., Vidal-Sanz, M., Lund, R.D., 1996. Mechanism of retinal ganglion cell loss in inherited retinal dystrophy. Neuroreport 7, 1995–1999.
Villegas-Perez, M.P., Vidal-Sanz, M., Rasminsky, M., Bray, G.M., Aguayo, A.J., 1993. Rapid and protracted phases of retinal ganglion cell loss follow axotomy in the optic nerve of adult rats. J. Neurobiol. 24, 23–36.
Wang, S., Villegas-Perez, M.P., Holmes, T., Lawrence, J.M., Vidal-Sanz, M., Hurtado-Montalban, N., Lund, R.D., 2003. Evolving neurovascular relationships in the RCS rat with age. Curr. Eye Res. 27, 183–196.
Wessendorf, M.W., 1991. Fluoro-Gold: composition and mechanism of uptake. Brain Res. 553, 135–148.
Whiteley, S.J., Sauve, Y., Aviles-Trigueros, M., Vidal-Sanz, M., Lund, R.D., 1998. Extent and duration of recovered pupillary light reflex following retinal ganglion cell axon regeneration through peripheral nerve grafts directed to the pretectum in adult rats. Exp. Neurol. 154, 560–572.